Available online at www.sciencedirect.com
ScienceDirect
Journal of Geodynamics 42 (2006) 1–11
JOURNAL OF GEODYNAMICS
http://www.elsevier.com/locate/jog

Impact of a precise geoid model in studying tectonic structures—A case study in Iran

R. Kiamehr [a,b,*], L.E. Sjöberg [a]

[a] *Division of Geodesy, Royal Institute of Technology, SE-100 44 Stockholm, Sweden*
[b] *Department of Geomatics, Zanjan University, 313 Zanjan, Iran*

Received 8 September 2005; received in revised form 9 March 2006; accepted 8 April 2006

Abstract

Iran is one of the most active regions in the world with respect to earthquakes and tectonic motions in the lithosphere. In order to study the impact of the geoid model in detecting plate tectonic boundaries and in the establishment of an accurate height datum for future geodynamic observations, a new combined gravimetric geoid model for Iran (IRG04C) was computed by the method of least squares modification of Stokes formula based on the most recent gravity anomaly database, SRTM high resolution Digital Elevation Model (DEM), GRACE GGM02 Global Geopotential Model and GPS/levelling data. The RMS fit of the new geoid model versus GPS/levelling data is 9 cm, which is a 10 times better fit compared to the most recent published gravimetric geoid model in the area. An integrated approach, combining gravity, geoid and seismology data as well as a digital elevation model, was used to find possible correlations between these parameters. Our investigation indicates that all earthquakes with magnitude over 6.0 in the Richter scale are located in areas with a geoid slope exceeding 7.5%. The study shows a significant correlation between the horizontal gradient of the geoid and plate tectonic activities.

Keywords: Lateral geoid slope; Plate tectonics; SRTM; GRACE; GPS/levelling; Iran

1. Introduction

The geoid is the fundamental surface that defines the figure of the Earth. It can be described as the equipotential surface of the Earth's gravity field, which agrees most closely with mean sea level in the open oceans and ignores the effects of semi-dynamic sea surface topography. Also, it is used in most countries as the reference surface of the national vertical datum.

Geoid signals can give important information about the underlying density structure of the earth, and it can be used to locate the source depth of mass anomalies. Geoid undulations have been used to constrain the viscosity structure of the mantle over the past 15 years (Hager, 1984; Cadek and Fleitout, 1999; Kido and Yuen, 2000). Longer wavelength geoids have the source in the lower mantle (Chase, 1979) and shorter wavelength anomalies are caused by heterogeneities in the lithosphere (Stunff and Ricard, 1995). Using spherical harmonic decomposition, one could use the geoid locally to study a particular area with short wavelength variations (Hwang et al., 1998), intermediate wavelengths with emphasis

* Corresponding author. Tel.: +46 8 790 73 69; fax: +46 8 790 73 43.
E-mail address: ramin@infra.kth.se (R. Kiamehr).

0264-3707/$ – see front matter © 2006 Elsevier Ltd. All rights reserved.
doi:10.1016/j.jog.2006.04.001

on the transition zone (Kido and Cadek, 1997) and long wavelengths probing into the deep mantle (Cazenave et al., 1989).

The importance of the geoid in geophysics and geodynamics has been recognised by the studies of the correlation between the geoid and deep-earth mass density anomalies (Bowin, 1983); the constraints provided by the geoid on mantle rheology and flow (Hager, 1984); correlation between the geoid and westward drift of the geomagnetic field (Khan, 1971) and correlation between the geoid and plate tectonic features and seismic tomography (Silver et al., 1988). The geoid variations extracted from satellite altimetry has very significantly contributed to the mapping of the sea floor topography and the discovery of numerous seamounts and mountain ridges below sea level. The small regional geoid signal as can be seen in satellite altimetry has even been utilized in prospecting for oil. Basically, the geoid can provide a complementary source of information in geodynamics research (Featherstone, 1997).

Although geoid data should be applicable to study lithospheric evolution, doing so has proved challenging. The expected signal associated with plate cooling should be small, because it reflects processes only in the upper hundred or so km of a 2900 km thick mantle, a difficulty compounded by the fact that the geoid is most affected by density anomalies at depth (Crough, 1979). Efforts to extract a plate cooling signal from geoid data have thus relied on taking the geoid slope, the gradient of the geoid in the direction of increasing lithospheric age, to reduce the long wavelength components (DeLaughter et al., 1999). These results indicate that the geoid can be used as a tool for studying the thermal evolution of oceanic lithosphere. Spatial band-pass filtering and formation of the geoid slope (in itself a spatial filter) can extract the age-dependent signal from the new, high-quality regional or ocean-wide geoid data. Also, the application of spatial filtering to the age derivative of the geoid, extracts an age dependent signal which reflects lithospheric thermal evolution (DeLaugher et al., 1999). The Wavelet analysis, known as E-max and k-max, is especially effective for detecting plate tectonic boundaries and ancient suture zones along with areas of strong non-isocratic gravitational potential due to high differential stress (Vecsey and Hier Majumder, 2003).

A number of dedicated satellite missions, i.e. CHAMP, GRACE and GOCE, is and will be available for gravity field determination from space. The main potential application of the gravity missions is that they provide us with powerful means to map the gravity field and to detect gravity and geoid changes caused by earthquakes, which have never been detected up to the present. A case study of the 1964 Alaska earthquake (Sun and Okubo, 1998) indicated that the gravity change could be detected on the earth surface by a super-conducting gravimeter even as far as 5000 km away. A geoid height change due to the earthquake could reach at 1.5 cm. Sabadini and Dalla (2005) estimated the peak-to-peak change of the geoid undulation caused by the 2004 Sumatra earthquake to 1.8 cm. Such gravity and geoid height changes are expected to be detectable by modern space techniques, such as satellite radar altimetry and gravity missions.

On the other hand, the use of high resolution and precise regional geoid models with GPS is also the key procedure to determining orthometric heights, which is the basic data for most regional geodynamic research. This is especially evident in large countries like Iran with active tectonics, in which areas of rough terrain the establishment of a levelling network, like in the Alborz and Zagros mountains in the north and west, is very tedious and time consuming. By combining it with the precise geoid model, the GPS technique can be used efficiently for any levelling project and to monitor the regional earth crustal movements.

This paper is mainly composed of two parts. In the first part we briefly explain the procedure and data that were used to construct the new hybrid precise geoid model for Iran (Kiamehr, 2006a) based on the least squares modification of Stokes' (LSMS) formula (Sjöberg, 1984, 1991, 2003a,b). In the second part we discuss the relation between the gravity field/geoid and geodynamics in the region.

2. Iranian precise combined geoid model based on the KTH approach (IRG04C)

The new Iranian gravimetric geoid model (IRG04) (Kiamehr, 2006a) was computed based on the KTH approach (Sjöberg, 2003a) with additive correction terms. The surface gravity anomalies and GGMs are used to determine approximate geoidal heights ($\tilde{N}$) and all necessary corrections are added directly to $\tilde{N}$ (see Eq. (2)). In other approaches, these corrections are usually computed one by one in separate corrections in steps, such that in the first step the surface gravity anomalies are corrected by removing the effects of topographic and atmospheric external masses (or reducing them below the geoid) as *direct effects*, and then, after applying Stokes integral, their effects are restored (*indirect effects*). In addition, the gravity anomalies in Stokes' formula must refer to the geoid, so that a reduction of the observed gravity from the Earth's surface to the geoid is necessary; that is called *downward continuation* (DWC). In the KTH approach,

all these separate effects are replaced by a *total topographic effect* (Sjöberg, 2001). The computational procedure for estimating the geoid height $\hat{N}$ in the KTH approach can be summarized by the following formula:

$$\hat{N} = \tilde{N} + \delta N_{\text{comb}}^{\text{Topo}} + \delta N_{\text{DWC}} + \delta N_{\text{comb}}^{\text{a}} + \delta N_{\text{e}} \tag{1}$$

where $\delta N_{\text{comb}}^{\text{Topo}}$ is the *combined topographic correction* and it includes the sum of direct and indirect topographical effects on the geoidal heights, δN_{DWC} the correction for the downward continuation effect (Sjöberg, 2003b), $\delta N_{\text{comb}}^{\text{a}}$ the *combined atmospheric correction* (Sjöberg, 2001) and it includes the sum of direct and indirect atmospherical effects, and δN_{e} is the ellipsoidal correction for the spherical approximation of the geoid in Stokes formula to ellipsoidal surface of reference. (For more details about these correction terms we refer to Kiamehr (2006a)).

The approximate geoid height ($\tilde{N}$) is computed based on the general modification model for Stokes' formula by defining two sets of arbitrary modification parameters (s_n and b_n) as follows:

$$\tilde{N} = \frac{c}{2\pi} \iint_{\sigma_0} S_L(\psi) \Delta\tilde{g} \, \mathrm{d}\sigma + c \sum_{n=2}^{M} b_n \, \Delta\tilde{g}_n^{\text{EGM}} \tag{2}$$

where $c = R/2\gamma$, $b_n = Q_n^L + s_n$, Q_n^L is the truncation coefficients' and it can be calculated by $Q_n^L = Q_n - \sum_{n=2}^{\infty} \frac{2k+1}{2} s_k e_{nk}$, where $Q_n = \int_{\psi_0}^{\pi} S(\psi) P_n(\cos\psi) \sin\psi \, \mathrm{d}\psi$, $e_{nk} = \int_{\psi_0}^{\pi} P_k(\cos\psi) P_n(\cos\psi) \sin\psi \, \mathrm{d}\psi$ and R is mean Earth radius, ψ is geocentric angle, $\Delta\tilde{g}$ is free gravity anomaly, $\mathrm{d}\sigma$ is an infinitesimal surface element of the unit sphere σ, and γ is the normal gravity on the reference ellipsoid. The modified Stokes' function is expressed as

$$S_L(\psi) = S(\psi) - \sum_{n=2}^{L} \frac{2n+1}{2} s_k P_k(\cos\psi) \tag{3}$$

where $S(\psi)$ is the Stokes' function, $P_n \cos(\psi)$ is the *Legendre* polynomial of degree n, and s_n are the least squares modification parameters (for more details see, Sjöberg, 1991). The upper limit L (in Eq. (2)) is arbitrary and generally not equal to M.

For the generation of the gravity database a total number of 26,125 point and mean gravity data were collected from different data sources (Kiamehr, 2005). Various databases including Bureau Gravimetrique International (BGI), National Cartographic Centre of Iran, original 0.5×0.5 degree surface free-air gravity anomaly data (that were used in the modelling of the EGM96) and satellite altimetry data (Sandwell and Smith, 1997) were used in this database. (For more details, see Kiamehr, 2005). Fig. 1 shows the distribution of the gravity data.

The final geoid model was computed based on free-air gravity anomalies in 80×90 seconds grid size, GGM02S (GRACE, 2004) global geopotential model and Shuttle Radar Topography Mission (SRTM) based

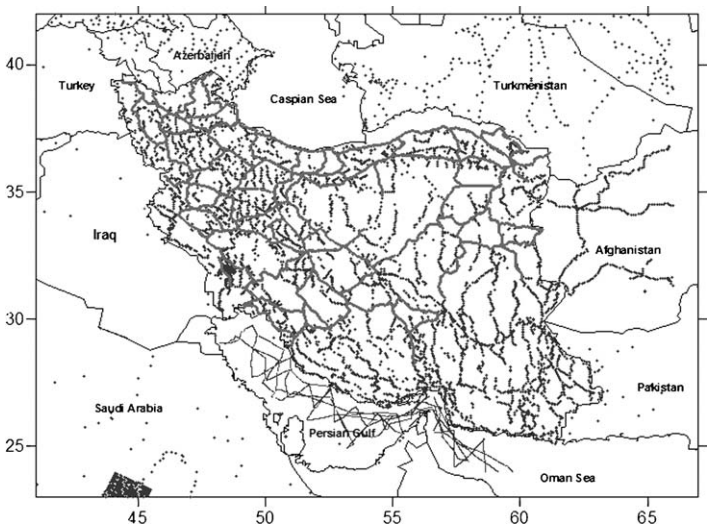

Fig. 1. Gravity anomalies data in the target area (including the new gravity observation (NCC) along the Iranian levelling network, BGI and ship-borne data in marines).

Table 1
Validation of the IRG04 and new combined geoid model vs. 35 GPS/levelling data (unit: m)

	Minimum	Maximum	Mean	RMS
IRG04 geoid gravimetric model	−1.284	0.223	−0.652	0.362
IRG04 after seven parameter fitting approach	−0.518	0.924	0.000	0.288
New combined model (IRG04C)	−0.474	0.433	0.000	0.088

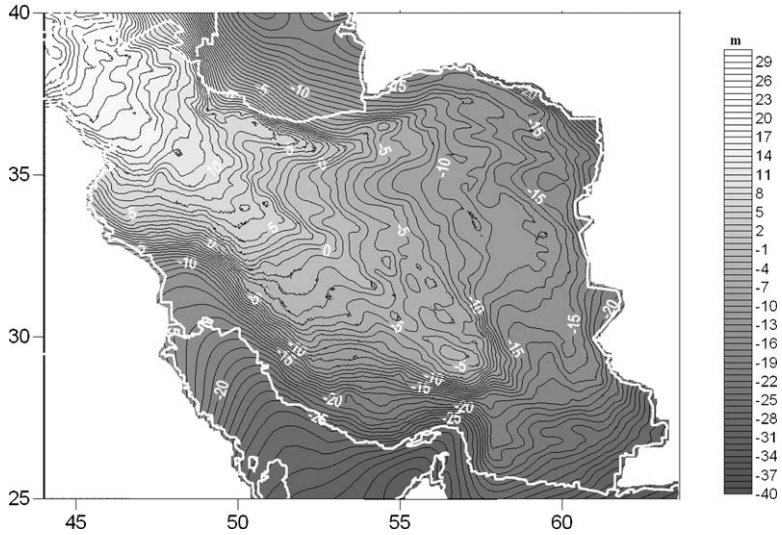

Fig. 2. The new Iranian combined geoid model (IRG04C). Contour interval is 2 m.

on a 100 m digital elevation model (Kiamehr and Sjöberg, 2005b). The full potential of the GGM02S (http://www.csr.utexas.edu/grace/gravity/) model with maximum degree and order of 110 (Kiamehr and Sjöberg, 2005a) was also used in determining the least squares modification parameters. The integral cap size three degrees and the pre-estimated accuracy for gravity data $\sigma_{\Delta g} = 10$ mGal (See Kiamehr, 2005 for more details) were used in estimating the modification parameters. For more information and details about IRG04 gravimetric geoid model see Kiamehr (2006a).

The absolute and relative accuracies of the new geoid model were tested versus the 35 precise GPS/levelling points, and the RMS of fitting between the IRG04 geoid model and GPS/levelling data evaluated before and after a seven parameter fitting reach 0.36 and 0.29 m, respectively (Kiamehr, 2006b). Also, in order to define a new height datum for Iran, we attempt to combine this high resolution gravimetric geoid model with GPS/levelling data by using a corrective surface idea (Kiamehr, 2006b).

Recently another gravimetric geoid model was published in this area (Safari et al., 2005), and the RMS of fitting of this model with the GPS/levelling data reported almost 1.07 m. Based on the result of Table 1, the IRG04 and its combined version (IRG04C) fit almost three times and 10 times better compared to the last mentioned gravimetric geoid model, respectively. Fig. 2 shows the contour map of the IRG04C geoid model. The new surface should therefore be more convenient and useful in defining a height datum for geodynamics and engineering projects.

3. Tectonic interpretation of the geoid

The Iran region is known as an extraordinary natural laboratory for the study of seismo-tectonic processes. This area is geologically and geophysically as well as geodetically one of the most studied regions on Earth. It is one of the regions that are located in the line of the most recent foldings along the length of the Alp strip in Europe to the Himalayas in the north of India. Here Iran is in the place of the junction of the Saudi Arabia, India and Eurasia plates. The junction of these plates has led to the seismicity of Iran, and, as a result, most regions and cities of Iran are exposed to frequent earthquakes.

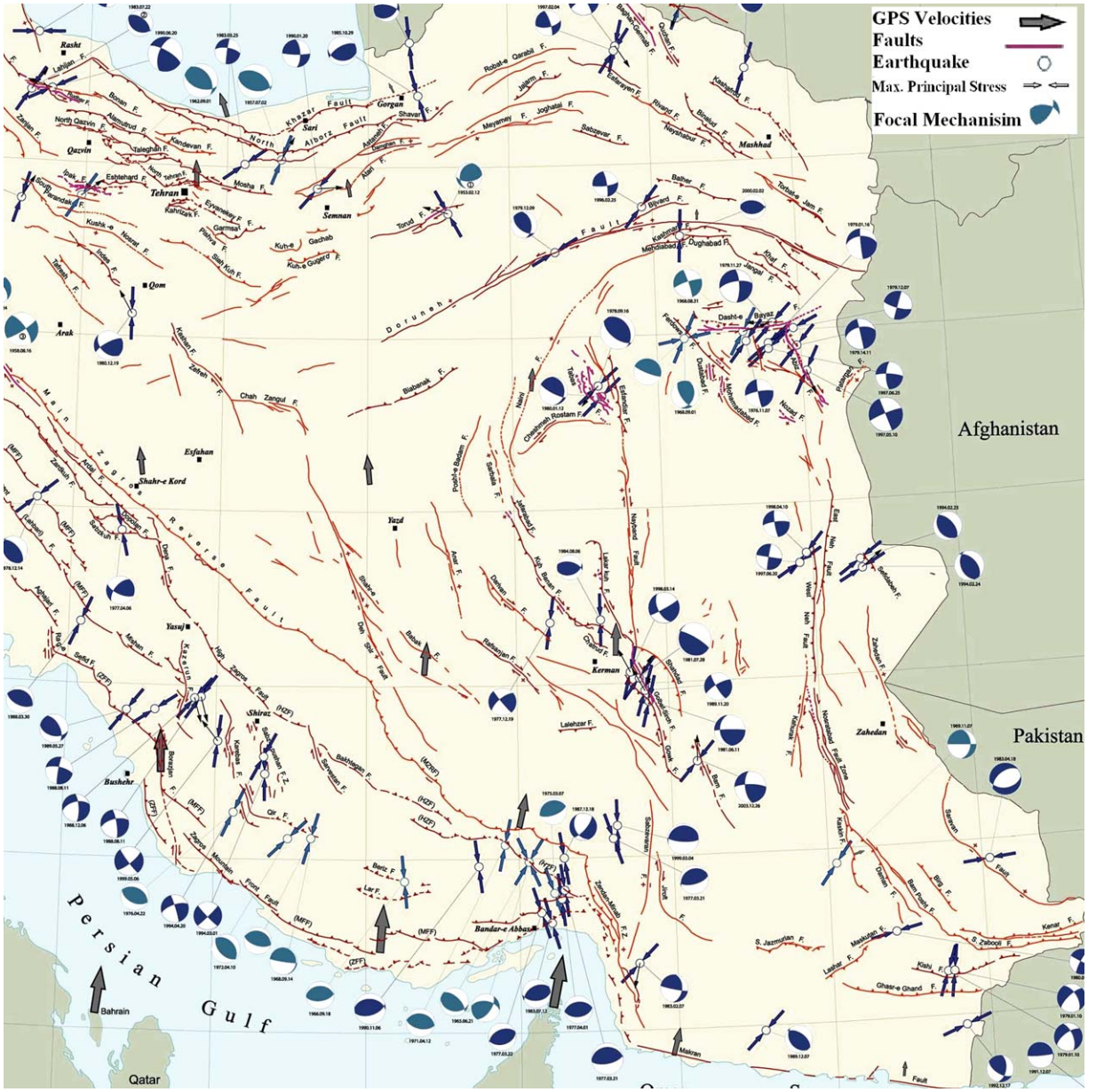

Fig. 3. The simplified structural map of central-east Iran showing the location of major faults. Large arrows indicate the direction of plate motion (http://www.iiees.ac.ir/Seismology/ActiveFault.pdf).

Much of the mechanical deformation resulting from the Arabia-Eurasian collision is accommodated by the Zagros ranges in the form of folding of rocks and the rise of mountains in conjunction with fault movements at depth of the Earth. In fact, the highest frequency of earthquakes in Iran occurs in the Zagros region (Fig. 3). The Zagros Mountains can be interpreted as being the final product of a geosynclinal cycle.

However, because of the diffuse nature of this deformation (i.e. simultaneous movements along a number of sub-parallel faults over a wide area) the intensities of these tremors are generally low and are recordable only by sensitive seismic devices. The interior parts of Iran, however, respond to the plate collisional forces in a different manner. In the area known as Central-East Iran deformation takes place largely in the form of strike-slip (sideway) movements focused along a complex array of intersecting faults (Fig. 3). In sharp contrast to that in Zagros, seismic activity associated with central Iranian faults is sporadic but much more localized and occurs with significantly higher magnitudes. Many

Table 2
Statistical analysis of the earthquakes in Iran (since 1902)

Number of data = 5900	Magnitude (Richter)	Geoid height N (m)	Depth D (km)	Height H (m)	Geoid slope NS (%)	Free-air anomaly Δg (mgal)	Bouguer anomaly Δg_B (mgal)
Minimum	1.70	−34.23	0.00	−47.03	0.25	−142.79	−317.538
Maximum	7.7	25.23	160.00	4627.11	23.99	274.22	52.683
Mean	4.15	−9.64	29.36	1091.50	8.18	9.67	−113.559
Standard deviation	0.84	11.62	16.26	771.98	4.51	65.89	43.546

of Iran's powerful tremors, such as the recent Bam earthquake, occurred in this area. Fig. 3 illustrates the major fault structures of the Central-East Iranian region along with large centres of population in their vicinity. Recent global plate models, constrained by GPS observations, show approximately a north-south shortening in eastern Iran, with rates of about 20 mm/year at 50_E and 26 mm/year at 60_E (Sella et al., 2002).

An integrated approach, combining the use of gravity, geoid, and topography and seismology data allows having a detail study of the crustal and lithospheric structure of the region. In the current study we used the most recent information, which come from the high resolution Shuttle Radar Topography Mission (SRTM), free air gravity grid database (Kiamehr, 2005) and the new precise combined geoid model (IRG04C), the complete earthquakes database of Iran, which was gathered by the International Institute of Earthquake Engineering and Seismology (IIEES). The seismological database has 5900 records and includes the general information of the earthquakes since 1902 (Table 2).

Fig. 4 shows the distribution of the seismologic data on the topographic map of Iran. Distribution of the earthquake data of Iran show that most activity is concentrated along the Zagros fold thrust belt while less activity is observed in central and eastern Iran. The topography of the tectonically active areas reflects recent tectonic processes. In particular, the topography associated with active faults must ultimately be related with the cumulative effect of the uplift and subsidence occurring in individual earthquakes. By visual comparison of the structural and topographic maps (see Figs. 3 and 4), we can see that there is a general correlation between topography and earthquake activates in Iran. Table 2 shows the statistical analysis of the extracted heights of the earthquake locations from the SRTM model. The mean height of the seismological database points is 1091 m, but the classification of earthquakes with the magnitude over six says that their mean height is 1275 m. We can conclude that the flat and moderate topographic areas (like as central of Iran) has a lower risk of earthquakes compared to the mountainous areas in the north and south-west. However, without independent information about the age of the topographic features, nothing can be said about the rates of processes that have created the present landscape.

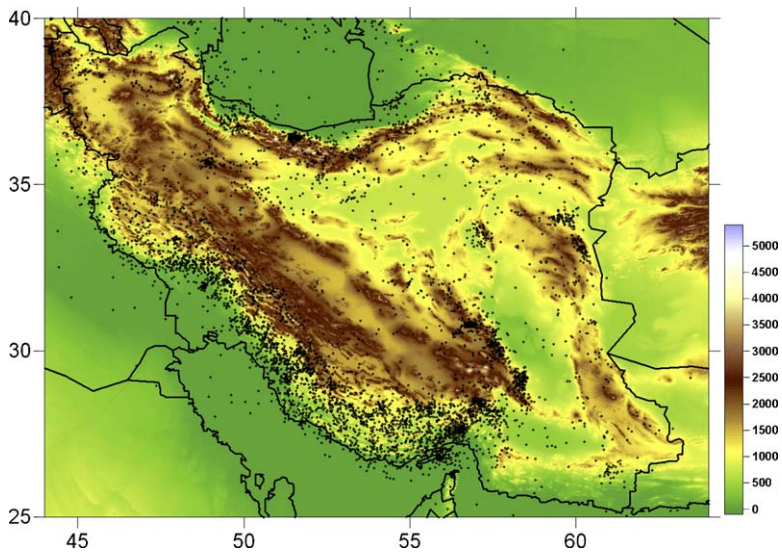

Fig. 4. Distribution of earthquakes (black dots) on digital elevation model of Iran (unit: m).

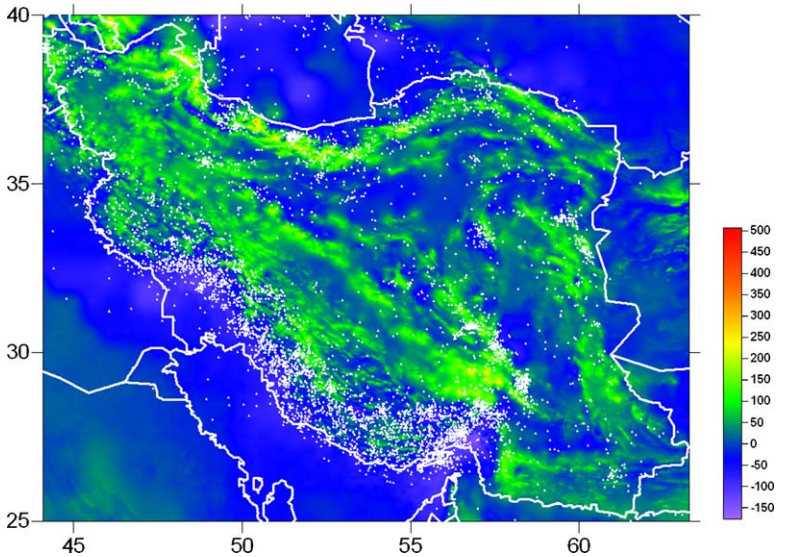

Fig. 5. Distribution of earthquakes (white dots) on the free-air anomaly grid (unit: mgal).

Also, a detail study of the thematic map of the free-air anomaly and the statistical analysis of the extracted values from the grid for the seismological data (see Fig. 5 and Table 2) clearly shows very local and complicated structures (like topography), which are mostly related with local mass variations and shallow density contrasts below sea level and could therefore be useful in studying local tectonic patterns.

The large positive anomalies in the Alborz and Zagros in Fig. 5 are interpreted to be a result of higher-density mantle lithosphere. This interpretation is based on the fact that strong structural variations in the crust are likely to be the source of this relatively uniform but widespread residual anomaly. The sediment thickness in the southern Caspian Sea is estimated to be about 20 km. In order to obtain such high gravity values above this region, higher density material must reside in the lower crust and/or in the upper mantle. Earlier studies have also indicated that this part of the Eurasian continent is underlain by a denser mantle lithosphere (Artemjev and Kaban, 1994). Combining these two observations, we conclude that higher-density material in the uppermost mantle is the likely candidate for the cause of this anomaly. However, as rule, a strong positive free-air anomaly with a weak Bouguer anomaly indicates a structure is supported by the strength of the lithosphere i.e. no compensation where a weak free-air anomaly with a strong negative Bouguer anomaly may indicate that the structure is compensated.

Similar to gravity, the geoid reflects mass variations in the Earth's interior of various wavelengths, but, in contrast to gravity, the geoid primarily reflects the long and medium wavelengths. Hence, it is more useful in studying global and regional mass anomalies in the Earth, such as deep lithosphere structures. Fig. 6 shows the three-dimensional map of the new precise geoid model of Iran and the distribution of the earthquakes. From the first view and in comparing with the simple structural map of Iran (Fig. 3), we can see that there is a clear correlation between the position of the main faults and the geoid undulations. This is particularly clear in the Zagros tectonic belt in the south.

Another interesting map for the geoid slope (gradient map of the geoid or geoid deflection map) clearly shows the presence of the significant correlation between the lateral geoid gradient and distribution of the earthquakes in Iran (see Fig. 7). Our statistical analysis shows that almost 72% of the earthquakes in Iran happened in the areas, which have geoid slope over 5%. The minimum, maximum, mean and standard deviation of earthquake magnitudes are 1.7, 7.7, 4.15 and 0.84 Richter, respectively. It is also interesting that all 78 earthquakes with magnitude over 6 Richter are located at the geoid slope 7.5% or more. Fig. 8 presents the histogram graphs of distribution of the earthquakes on topographic, free-air anomaly (Δg_{free}), geoidal height (N), lateral geoidal slope, earthquake depth and magnitude.

In order to give a better view about the presence of possible statistical correlation between different parameters, we determined the correlation value for all parameters as shown in Table 2. The coefficients are also compared with their critical values to be used in testing the significance of the estimated correlations. For a two-tailed test degree of freedom value is equal to d.f. $= n - 2$, where n is number of paired observations (in our case 5900). Based on the table of critical values for correlation (Cohen, 1988) with the significance level of $a = 0.05$, we got the critical value of r for

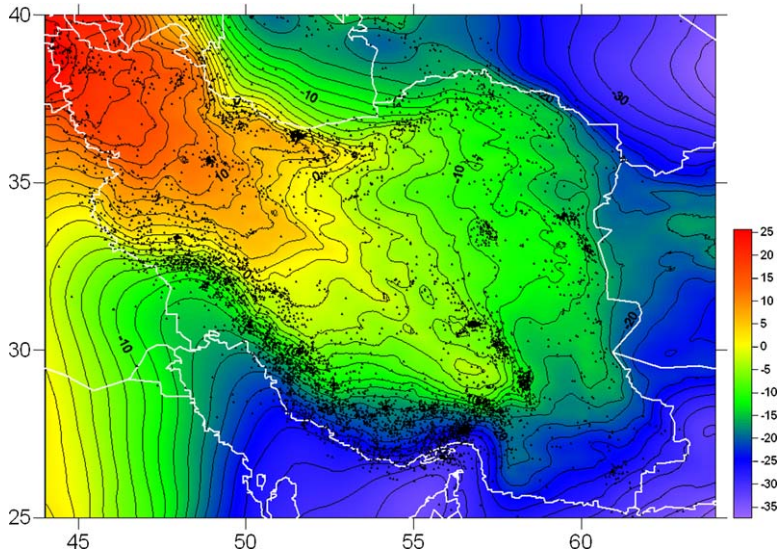

Fig. 6. A perspective view of the new Iranian combined geoid model (IRG04C). The distribution of earthquakes plotted with black dots (unit: m).

all parameters about ($r_{crit} = 0.062$), the maximum available n in table is 1000. We can conclude the following results from Table 3:

- All correlations are significant except those between NS and N as well as between NS and R.
- There is a strong correlation between topographic height and each of free-air anomaly and simple Bouguer anomaly.
- There is a positive and significant correlation between the geoid slope and earthquake depth parameter in the order of +0.46 in the Zagros area.
- There is a significant and remarkable correlation between the depth and magnitude of earthquakes in the study area ($r = 0.402$).
- The geoid slope parameter (NS) and free-air anomaly have the highest correlation value among different parameters with the depth of the earthquake (D). It could be an important sign from the earthquake study view. However, the

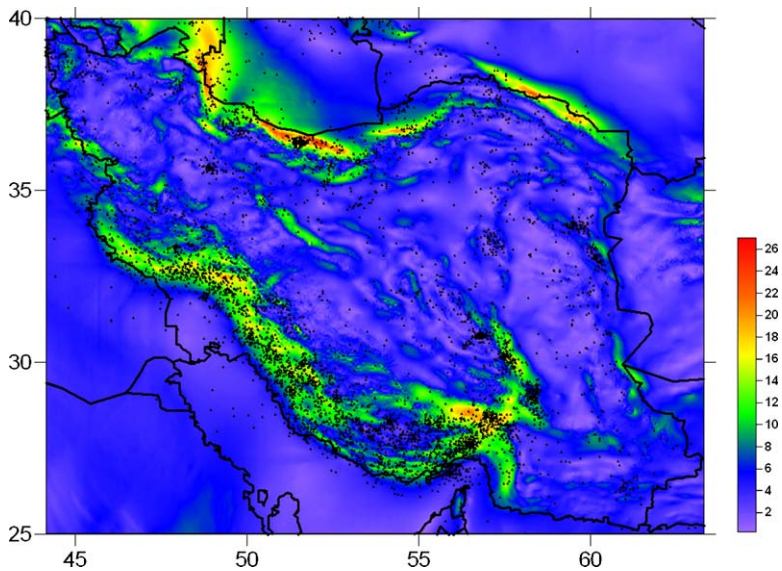

Fig. 7. Distribution of earthquakes (black dots) on the lateral geoid slope map (slope in percentage).

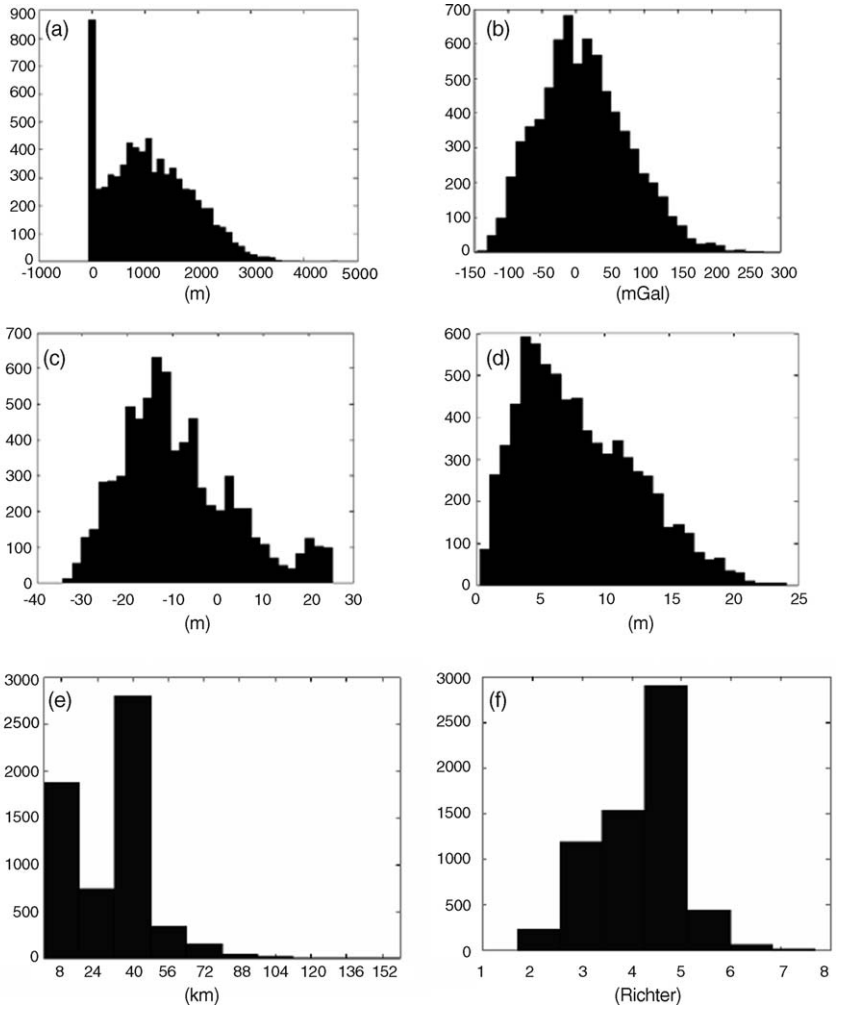

Fig. 8. Histogram graphs of distribution of the earthquakes on (a) topographic map, (b) free-air gravity anomaly (Δg_{free}), (c) geoidal height (N), (d) geoidal height slope, (e) earthquake depth and (f) earthquake magnitude.

gravity anomaly is a differential quantity, so it exhibits small scale structure where the geoid is an integrated quantity, so it is optimal for studying long wavelength effects and major tectonic features. We think that the information from the simple and clear map of the geoidal slope and the complicated map of the free-air anomaly are complemantary for the local and regional interpretations of earthquakes and plate tectonics.

Table 3
Correlation values between different parameters in this study

Parameters/ correlation	Height (H)	Geoid height (N)	Geoid slope (NS)	Free-air anomaly (Δg_{free})	Bouguer anomaly (Δg_{B})	Earthquake magnitude Richter (R)	Earthquake depth (D)
H	1	+0.502	−0.124	0.867	−0.615	−0.156	−0.130
N	0.502	1	0.013	0.460	−0.280	−0.147	−0.080
NS	−0.124	0.013	1	−0.080	0.120	0.015	0.132
Δg_{free}	0.867	0.460	−0.080	1	−0.176	0.122	−0.133
Δg_{B}	−0.615	−0.280	0.120	−0.176	1	0.119	0.067
R	−0.156	−0.147	+0.015	0.122	0.119	1	0.402
D	−0.130	−0.080	+0.134	−0.133	0.067	0.402	1

4. Conclusion

In this study a new, combined gravimetric geoid model for Iran (IRG04C) has been computed. The RMS fit of the combined geoid model versus GPS/levelling data is estimated to 9 cm, which is 10 times smaller than the fit for the most recent published gravimetric geoid model in this area.

An integrated approach, including geophysical and geodetic data, such as topography, free-air anomaly, geoid, and seismological data, was used to study possible correlations between the earthquake frequency and other parameters, and we have shown a significant correlation between the lateral geoid variation/slope and earthquake/tectonic activities. The statistical analysis shows that 72% of the earthquakes in Iran occurred in areas, which have a lateral geoid slope of at least 5%. Also, all earthquakes with magnitudes over six are located in areas with geoid gradients exceeding 7.5%. This new result calls for a more detailed determination of the deflections of the vertical and its correlation with earthquake activities, both in Iran and in other tectonically active regions of the world.

Acknowledgements

The authors are grateful to Mr. Naeim Dastgir for his kind support in the construction of the different models in a GIS platform. Part of the gravity anomaly and the GPS/levelling data used in this research was prepared by the National Cartographic Centre and the International Institute of Earthquake Engineering and Seismology (IIEES) of Iran. Special thanks go to Professors Giorgio Ranalli and Wolf Jacoby as well as to an unknown reviewer for their valuable suggestions and comments to a previous version of the manuscript.

References

Artemjev, M.E., Kaban, M.K., 1994. Density inhomogeneities, isostasy and flexural rigidity of the lithosphere in the transcaspian region. In: Cloetingh, S., Eldholm, O., Larsen, B.T., Gabrielsen, R., Sassi, W. (Eds.), Dynamics of Extensional Basin Formation and Inversion. Tectonophysics 240, 281–297.

Bowin, C.O., 1983. Depth of principal mass anomalies contributing to the Earth's geoidal undulations and gravity anomalies. Mar. Geod. 7, 61–100.

Cadek, O.P., Fleitout, L., 1999. A global geoid model with imposed plate velocities and partial layering. J. Geophys. Res. 104 (B12), 29055–29075.

Cazenave, A., Souriau, A., Domiah, K., 1989. Global coupling of Earth surface topography with hotspots, geoid and mantle heterogeneities. Nature 340, 54–57.

Chase, C.G., 1979. Subduction, the geoid, and lower mantle convection. Nature 282, 464–468.

Cohen, J., 1988. Statistical Power Analysis for the Behavioral Sciences. Lawrence Erlbaum Assoc., Hillsdale, NJ, ISBN 0805802835.

Crough, S., 1979. Geoid anomalies across fracture zones and the thickness of the lithosphere. Earth Planet. Sci. Lett. 44, 224–230.

DeLaughter, J., Stein, S., Stein, C., 1999. Extraction of a lithospheric cooling signal from oceanwide geoid data. Earth. Planet. Sci. Lett. 174, 173–181.

Featherstone, W.E., 1997. On the use of the geoid in geophysics: a case study over the north-west shelf of Australia. Expl. Geophys. 28 (1), 52–57.

GRACE, 2004. GRACE Gravity Model GGM02. University of Texas at Austin, Center for Space Research. http://www.csr.utexas.edu/grace/gravity/.

Hager, B.H., 1984. Subducted slabs and the geoid: constraints on mantle rheology and flow. J. Geophys. Res. 89, 6003–6016.

Hwang, C., Kao, E.-C., Parsons, B., 1998. Global derivation of marine gravity anomalies from Seasat, Geosat, ERS-1 and TOPEX/POSEIDON altimeter data. Geophys. J. Int. 134, 449–459.

Kiamehr, R., 2005. Qualification and refinement of the Iranian gravity database. In: NCC Geomatics 84 Conferences, Tehran, Iran.

Kiamehr, R., 2006a. A strategy for determining the regional geoid by combining limited ground data with satellite-based global geopotential and topographical models: a case study of Iran. J. Geod. 79 (10/11), 602–612.

Kiamehr, R., 2006b. A new height datum for Iran based on combination of the gravimetric and GPS/levelling geoid models. IAG Symposia Series by Springer Verlag, Dynamic Planet 2005 Conference, 22–26 August 2005, Australia, Cairns.

Kiamehr, R., Sjöberg, L.E., 2005a. The qualities of Iranian gravimetric geoid models versus recent gravity field missions. J. Stud. Geophys. Geod. 49, 289–304.

Kiamehr, R., Sjöberg, L.E., 2005b. Effect of the SRTM global DEM in the determination of a high-resolution geoid model of Iran. J. Geod. 79 (9), 540–551.

Kido, M., Cadek, O., 1997. Inferences of viscosity from the oceanic geoid: indication of a low viscosity zone below the 660-km discontiuity. Earth Planet. Sci. Lett. 151, 125–138.

Kido, M., Yuen, D.A., 2000. The role played by a low viscosity zone under a 660 km discontinuity in regional mantle layering. Earth Planet. Sci. Lett. 181, 573–583.

Khan, M.A., 1971. Some geophysical implications of the satellite-determined geogravity field. Geophys. J. Roy. Astron. Soc. 23, 15–43.

Sabadini, R.S., Dalla, G., 2005. A splash in Earth gravity from the 2004 Sumatra earthquake. EOS 86 (15), 151–153.

Safari, A., Ardalan, A.A., Grafarend, E.W., 2005. A new ellipsoidal gravimetric, satellite altimetry and astronomic boundary value problem, a case study: the geoid of Iran. J. Geodyn. 39, 545–568.

Sandwell, D.T., Smith, W.H.F., 1997. Marine gravity anomaly from Geosat and ERS 1 satellite altimetry. JGR 102 (B5), 10039–10054.
Sella, G.F., Dixon, T.H., Mao, A., 2002. REVEL: a model for recent plate velocity from space geodesy. J. Geophys. Res. 107, doi:10.1029/2000JB000033.
Silver, P.G., Carlson, R.W., Olson, P., 1988. Deep slabs, geochemical heterogeneity and the large scale structure of mantle convection: investigation of an enduring paradox. Earth Planet. Sci. Lett. 16, 477–541.
Sjöberg, L.E., 1984. Least squares modification of Stokes' and Vening Meinesz' formulas by accounting for truncation and potential coefficient errors. Manuscr. Geod. 9, 209–229.
Sjöberg, L.E., 1991. Refined least squares modification of Stokes' formula. Manuscr. Geod. 16, 367–375.
Sjöberg, L.E., 2001. Topographic and atmospheric corrections of gravimetric geoid determination with special emphasis on the effects of degree zero and one. J. Geod. 75, 283–290.
Sjöberg, L.E., 2003a. Improving modified Stokes' formula by GOCE data. Bull. Geod. Sci. Aff. 61 (3), 215–225.
Sjöberg, L.E., 2003b. A computational scheme to model the geoid by the modified Stokes formula without gravity reductions. J. Geod. 74, 255–268.
Stunff, Y., Ricard, Y., 1995. Topography and geoid due to lithospheric mass anomalies. Geophys. J. Int. 122, 982–990.
Sun, W., Okubo, S., 1998. Surface potential and gravity changes due to internal dislocations in a spherical earth. Geophys. J. Int. 132, 79–88.
Vecsey, L., Hier Majumder, C.A., 2003. Multiresolution tectonic features over the Earth inferred from a wavelet transformed geoid. Vis. Geosci. 8, 26–44.